Piezothermal effect in a spinning gas

V. I. Geyko and N. J. Fisch

Department of Astrophysical Sciences, Princeton University, Princeton, New Jersey 08544, USA

A spinning gas, heated adiabatically through axial compression, is known to exhibit a rotation-dependent heat capacity. However, as equilibrium is approached, an effect is identified here wherein the temperature does not grow homogeneously in the radial direction, but develops a temperature differential with the hottest region on axis, at the maximum of the centrifugal potential energy. This phenomenon, which we call a *piezothermal effect*, is shown to grow bilinearly with the compression rate and the amplitude of the potential. Numerical simulations confirm a simple model of this effect, which can be generalized to other forms of potential energy and methods of heating.

I. INTRODUCTION

A spinning gas exhibits a rotation-dependent heat capacity [1]. Under axial compression, a cylinder of gas rotating about its axis will become hotter, but not as hot absent the rotation. This effect occurs because, as the gas becomes hotter, gas molecules originally flung by centrifugal forces to the periphery become more homogeneously distributed. Since the heating changes the moment of inertia, the gas must spin faster to conserve angular momentum. Thus, some of the energy expended in compressing the gas goes to making the gas rotate faster, rather than into heating it, making it softer to compress axially. The question now posed is as follows: To the extent that the axial compression is not quite infinitely slow, do radial temperature gradients develop?

We identify here that, in fact, radial temperature gradients do develop in the direction perpendicular to the gas compression. By analogy with the piezoelectric effect [2], we term this temperature gradient formation a *piezothermal effect*. It will become clear how, in certain limits, this analogy is rather precise. The effect appears in the presence of any potential. With compression perpendicular to the potential gradient, temperature gradients arise in the direction of the potential gradient.

Although our interest is spinning gas in a cylinder, for didactic purposes, consider first a slab of gas in equilibrium in a vertical gravitational field, so that it has an atmospheric density distribution but constant temperature. The force of gravity takes the place of the centrifugal force, but, since gravity is constant, rather than coupled to temperature, the essential effect is captured far more simply. If the slab is compressed slowly in the horizontal direction, it becomes hotter, so the scale height rises. For a mean free path that is small compared to system size, at each height local thermodynamic equilibrium is achieved. As the gas becomes hotter, an axial temperature gradient develops, with the gas on bottom coldest. This is the piezothermal effect in a gravitational field.

There are several important time scales: the collision time τ_c, the compression or energy input time τ_E, the rise time of the gas or sound time τ_s, and the heat diffusion time τ_H. Consider the case $\tau_c \ll \tau_E \ll \tau_s \ll \tau_H$. The smallness of τ_c guarantees local thermodynamic equilibrium. The largeness of τ_H allows for temperature differentials. The inequality $\tau_E \ll \tau_s$ means fast compression, where the energy from compression will first be distributed among all other degrees of freedom, while the density remains unchanged. Although more energy is

deposited at the bottom than at the top, the energy deposited per particle is the same throughout the vertical direction, since the energy delivered to the particles is just proportional to the particle number at that height. Local thermodynamic equilibrium is achieved at increased temperature, but the system is not in global equilibrium, so the gas center of mass (c.m.) rises to the proper scale height. Particles on the bottom then see a receding c.m. *ceiling*, and hence are cooled by collisions with the receding ceiling; conversely, particles on top see a rising c.m. *floor*, and hence are heated. In the following, these predictions will be described quantitatively and demonstrated through simulations.

Similarly, the axial compression of spinning gas produces a piezothermal effect. Here the temperature in the center is higher than at the periphery, since the centrifugal force pushes from the center to the periphery. Interestingly, the fact that the hottest region is on axis might be useful in low-temperature engines with spinning gas, either by initiating a central spark or by limiting energy loss at the periphery. This temperature differential occurs in addition to the rotation-dependent heat capacity effect, which was already shown to increase the theoretical maximum of efficiency of internal combustion engines that utilize spinning gas [3].

That the temperature on axis tends to be larger than at the periphery might come as a surprise, since the effect is opposite to that in the Ranque-Hilsch vortex tube [4], a closely related rotating gas device. In the vortex tube, a very substantial radial temperature differential similarly occurs; however, the colder gas exits at small radii, while, in our case, the colder gas is found at larger radii. The source of the vortex tube temperature differential is still debated within the archival literature; explanations involve turbulence [5] or secondary flows [6]. The compression of spinning gas has been studied in other contexts as well, including vortex compression [7,8], the cutting of vortices [9], or under periodic compression, where a parametric instability appears [10]. However, it is the curious behavior of vortex tubes, in giving the opposite result, that most contributes to the surprise here.

II. GRAVITATIONAL POTENTIAL

To describe quantitatively the piezothermal effect, consider a slab of finite width (in the $\hat{x}$ direction) of an ideal gas in constant vertical gravitational field $-g\hat{z}$. In equilibrium, the
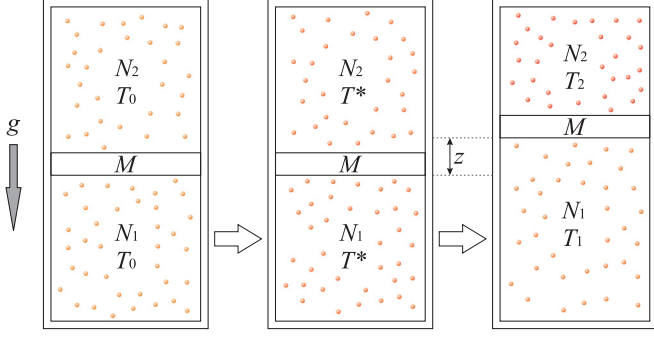
FIG. 1. Piezothermal effect. Step 1: equilibrium at T_0. Step 2: instant vertically uniform temperature rise to T^* produced by lateral compression. Step 3: pressure balance, under heat insulation, restored through partition displacement z.

temperature T is constant, so the density falls off exponentially, $n(z) = n_0 \exp(-z/\lambda)$, where z is the vertical height and $\lambda = T/mg$ is the atmospheric scale height, for particle mass m. Under adiabatic compression in the $\hat{x}$ direction, the gas c.m. rises, as the temperature increases. The increase in the gravitational potential energy causes the gravity-dependent heat capacity of the gas [11].

As will be demonstrated in particle simulations, the key piezothermal effects can be described in various limits by crudely modeling the gas, initially at temperature T_0, as divided by a movable, heat-insulating partition with mass M (later identified with the total gas mass), with N_1 massless molecules in the lower section and N_2 in the upper section, as depicted in Fig. 1. Consider first the case $\tau_E \ll \tau_s \ll \tau_H$, namely where sudden lateral compression heats the gas in a time τ_E short compared to the rise time τ_s. The initial pressure balance gives

$$N_1 T_0 / L_1 - N_2 T_0 / L_2 = Mg, \tag{1}$$

where $L_{1,2}$ are the lengths of the lower and upper sections respectively. Upon heating, the temperature increases everywhere from T_0 to T^*. To balance pressures, the partition rises to height z, but gas in the lower section performs mechanical work, and hence is cooled, while gas in the upper section is compressed and heated. Since $\tau_s \ll \tau_H$, the temperatures on top and bottom separately equilibrate to T_2 and T_1 respectively. For heat capacity c_v and heat capacity ratio γ, energy balance gives

$$c_v(N_1 T^* + N_2 T^*) = c_v(N_1 T_1 + N_2 T_2) + Mgz, \tag{2}$$

while the adiabatic law for each section gives

$$T_1 = T^*(1 + z/L_1)^{1-\gamma}, \quad T_2 = T^*(1 - z/L_2)^{1-\gamma}. \tag{3}$$

Equation (2) together with Eq. (3) is a transcendental equation for z; however, for small $z/L_{1,2}$, we can Taylor expand to second order and obtain the following solution:

$$z = \frac{2Mg\left(\frac{1}{T_0} - \frac{1}{T^*}\right)}{\gamma\left(\frac{N_1}{L_1^2} + \frac{N_2}{L_2^2}\right)}. \tag{4}$$

To estimate the magnitude of the temperature differential $T_2 - T_1$, we Taylor expand again Eq. (3) and make use of
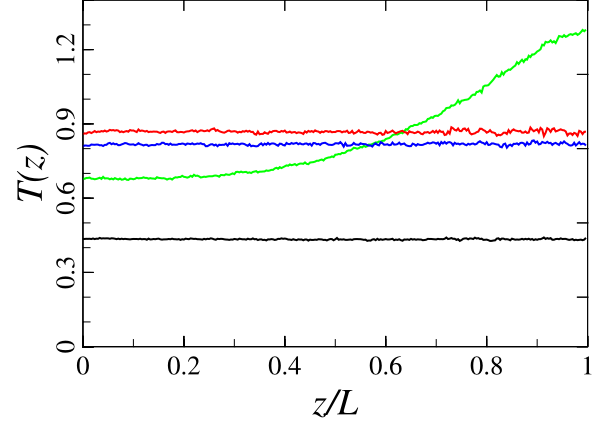

FIG. 2. Temperature profile for fast heating. Black: initial profile; red: upon heating; green: at maximum temperature gradient; blue: at new equilibrium. ($\delta = G = 1.0$.)

the expression for z from Eq. (4):

$$\Delta T = T_2 - T_1 = (\gamma - 1)zT^*\left(\frac{1}{L_1} + \frac{1}{L_2}\right)$$

$$= \frac{2(\gamma - 1)Mg\left(\frac{1}{L_1} + \frac{1}{L_2}\right)\left(\frac{T^*}{T_0} - 1\right)}{\gamma\left(\frac{N_1}{L_1^2} + \frac{N_2}{L_2^2}\right)}. \tag{5}$$

Now for large-scale heights $L \ll \lambda$, we can approximate $L_{1,2} \approx L/2$, $N_{1,2} \approx N/2$. For rough scaling, take the mass of the partition equal to the mass of the gas $M \approx Nm$, and expand for small displacements z/L, to find

$$\frac{\Delta T}{T_0} = \kappa_1\left(\frac{mgL}{T_0}\right)\left(\frac{T^* - T_0}{T_0}\right), \tag{6}$$

which exhibits bilinear dependence on $G = mgL/T_0 \equiv L/\lambda$, which measures the system size to scale height, and $\delta = (T^* - T_0)/T_0$, which measures the heat imparted, with proportionality constant $\kappa_1 = 0.8$ for monatomic ideal gas ($c_v = 3/2$, $\gamma = 5/3$).

Numerical simulations confirm these effects also in the absence of a partition. We used the direct simulation Monte Carlo method [12] in one-dimensional (1D) geometry in the vertical direction. A fluid code would also have captured the piezothermal effects. The fast heating or compression in the perpendicular direction was modeled by imparting to all particles, in a vertical column, a lateral impulse proportional to their lateral velocity. For hard-sphere collisions, the temperature first increases quickly and vertically uniformly. A temperature differential then develops, as depicted in Fig. 2. This differential is accompanied by a rise in the density scale height, as depicted in Fig. 3. The bilinear dependence on both G and δ in Eq. (6) is confirmed, with proportionality constant $\kappa_1 \approx 0.64$ numerically determined, by fitting a large number of particle simulations. The temperature gradient oscillates at the sound frequency. As the new equilibrium is reached, these oscillations are damped somewhat sooner than the heat diffusion time, $\tau_H \approx \nu_c L^2/v_t^2$, for thermal speed v_t, collision frequency $\nu_c = v_t n d^2$, and molecule radius d.

Interestingly, in the limit $L/\lambda \to \infty$, the temperature differential can no longer depend on L, since there are no
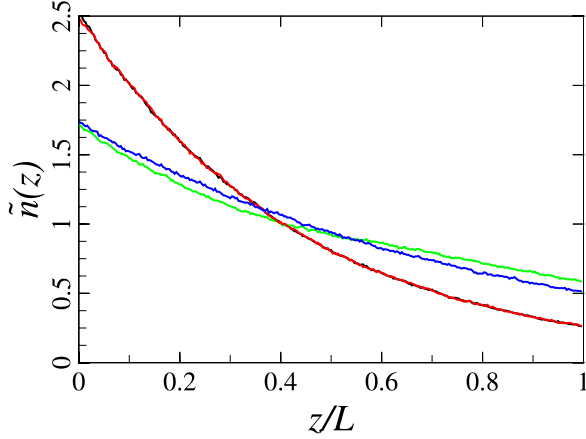
FIG. 3. Density profile for fast heating. Black: initial profile; red: upon heating; green: at maximum temperature gradient; blue: at new equilibrium. ($\delta = G = 1.0$.) Density is normalized to homogeneous one, i.e., total number of particles over total volume.

particles at large L. Hence, the bilinear dependence derived in Eq. (6) must be replaced by a dependency only on δ. However, at the same time, the notion of temperature becomes ill defined for too many scale heights. Focusing then on the temperature differential say between $z = 0$ and $z = c\lambda$, where $c \equiv \ln 10$, one determines through simulations $\Delta T / T_0 = 0.47\delta$. Note that the maximum temperature differential may occur at larger scale heights, but because of the increasing rare atmosphere, further contributions to the differential become less meaningful with greater heights.

Note that in either limit the temperature differential can be of the order of the temperature increase itself. To be concrete, consider for example a 100-m-high chamber, filled with xenon gas at 273 K. At standard gravity, a 10 K temperature differential results upon compression sufficient to heat to 546 K, assuming the compression time is less than the sound time of about 1 s. The heat diffusion time is about 10^9 s. Greater differentials are possible with realizable centrifugal forces. Spinning xenon gas at 30 000 rpm in a cylinder of radius 10 cm, and then heating it (like through axial compression) from $T = 273$ K to $T = 1355$ K, gives a temperature differential of 120 K between the axis and the periphery. This example is in the range of temperatures for low-temperature combustion engines [13]. For conventional engines, the maximum temperature is about 2200 K [14], so the temperature differential will be even greater. For the 10-cm engine, the sound time is about 0.7 ms, making 30 000 rpm marginally in the range of validity of Eq. (6). The heat diffusion time (about 10^3 s) is easily long enough.

III. SLOW COMPRESSION

For compression times exceeding the sound time, namely the case $\tau_c \ll \tau_s \ll \tau_E \ll \tau_H$, one might speculate that, once a temperature differential develops upon compression, namely after some change in the scale height, further lateral compression accentuates that differential. After all, compression heats at each height proportionally to the local vertical temperature, so less energy will go to the cooler regions. On the other

hand, slower heating means slower rise times, which would counteract this effect. It turns out, however, that, except for lateral compression $x(t)$ specifically timed to exploit the oscillations in temperature, slower compression produces smaller temperature differentials.

To see this, note that compression slow compared to sound time implies pressure balance as in Eq. (1), while temperatures of lower and upper sections read as

$$
T_{1,2} = T_0 \left[\frac{x(t)}{x_0} \left(1 \pm \frac{z}{L_{1,2}} \right) \right]^{1-\gamma}. \tag{7}
$$

Now make use of the temperature dependence and substitute it into the force balance equation Eq. (1). Then, for small z, obtain

$$
\bar{z} = \frac{(\eta - 1) M g}{\gamma T_0 \eta \left(\frac{N_1}{L_1^2} + \frac{N_2}{L_2^2} \right)}. \tag{8}
$$

Here $\eta = [x(t)/x_0]^{1-\gamma}$, and a bar over z denotes its smooth, averaged value, because in principal it will have a small quiver part that can be solved for but which is not needed for our analysis. From energy conservation, we see that the compression energy went to increase of temperatures of both sections of the gas, as well as to increase of the potential energy of the piston. Hence, we have

$$
Q = M g \bar{z} + c_v N_1 T_0 \left[\frac{x(t)}{x_0} \left(1 + \frac{\bar{z}}{L_1} \right) \right]^{1-\gamma}
$$
$$
+ c_v N_2 T_0 \left[\frac{x(t)}{x_0} \left(1 - \frac{\bar{z}}{L_2} \right) \right]^{1-\gamma}. \tag{9}
$$

Thus, Eq. (9) gives us an approximate relation between the normalized horizontal displacement η and the total amount of work Q. We can find the approximate expression for η as

$$
\eta = \frac{Q}{c_v T_0 (N_1 + N_2)} + 1. \tag{10}
$$

Substitute Eq. (10) into Eq. (8) to get $\bar{z}$ and then use it to find the normalized temperature differential,

$$
\frac{\Delta T}{T_0} = \frac{(T_2 - T_1)}{T_0}
$$
$$
= \frac{(\gamma - 1)}{\gamma} \left(\frac{1}{L_1} + \frac{1}{L_2} \right) \frac{M g Q}{T_0 Q_0 \left(\frac{N_1}{L_1^2} + \frac{N_1}{L_1^2} \right)}, \tag{11}
$$

where we denoted $Q_0 = c_v T_0 (N_1 + N_2)$. As we can see, in the case of continuous energy deposition, the final temperature difference has the same bilinear form as Eq. (6), with half the proportionality constant. However, by fitting numerical simulations of monatomic gas, we find numerically a slightly smaller proportionality constant, namely $\Delta T / T_0 = 0.26\,G\delta$. This indicates that, unless a very specific compression time profile is taken, compressing slower than the sound time gives a smaller temperature differential compared to compressing faster. Also keep in mind that this derivation was based on the assumption of small piston displacement; the result may be different in the case of extreme values of the parameters Q/Q_0 or mgL/T_0.
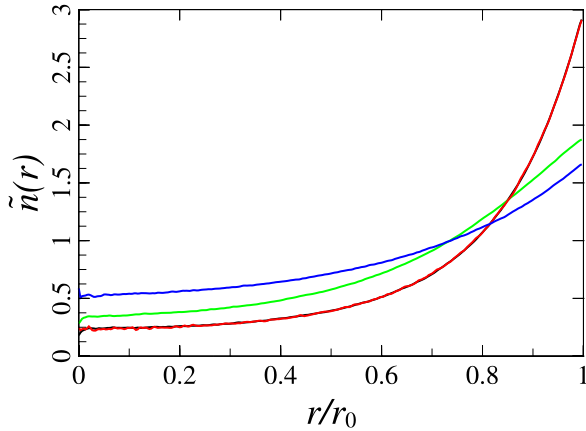
FIG. 4. Spinning gas normalized density profile. Black: initial profile; red: upon heating; green: at maximum temperature gradient; blue: new equilibrium. (Fast heating; $\delta = 8/3$; $\varphi_0 = 2.74$.)
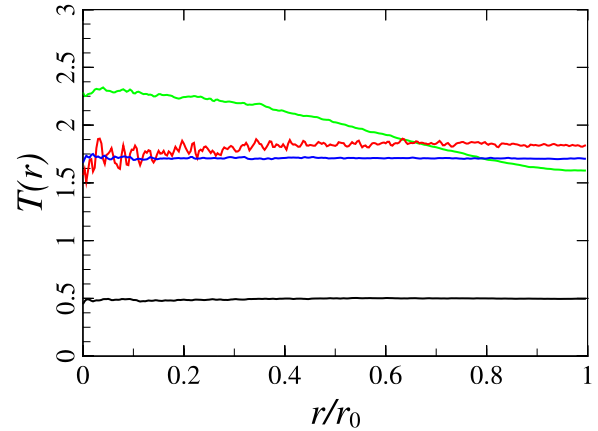

FIG. 5. Spinning gas temperature profile. Black: initial profile; red: upon heating; green: at maximum temperature gradient; blue: new equilibrium. (Fast heating; $\delta = 8/3$; $\varphi_0 = 2.74$.)

IV. CENTRIFUGAL POTENTIAL

The piezothermal effect under a centrifugal potential is considerably more complicated than under a gravitational potential because the temperature is coupled to the centrifugal potential. However, by analogy to the gravitational potential case, it can be expected that the temperature differential will be bilinear in the heat imparted through compression and the initial centrifugal potential parameter $\varphi_0 = m\omega^2 r_0^2/2T$. To see the analogous evolution effects, a spinning gas is simulated, with ignorable axial and azimuthal coordinates, and with specular reflection off the perfectly cylindrical boundary. The collision operator exploited the azimuthal symmetry to allow for hard-sphere collisions based on radial location only. The axial compression on a time scale short compared to a sound time is simulated by taking $v_z \rightarrow \alpha v_z$ for all particles, where z is the axial direction. As in the gravitational case, the imparted energy quickly becomes isotropic and thermally distributed, followed by radial density redistribution and a radial temperature differential. The collisions ensure that the system remains at all times very close to solid body rotation, even as the temperature and density evolve radially. Like in the 1D gravitational piezothermal effect, the temperature gradient in this limit oscillates several times before the new equilibrium is reached. In Fig. 4 the density evolution is shown. In Fig. 5, the temperature differential forms very much like in the case depicted in Fig. 2. As anticipated, the hotter region is near the axis. Note, however, that the region close to $r = 0$ is very noisy, since, for the centrifugal potential, there are very few particles on axis. Nonetheless, it can clearly be seen that a significant temperature differential is established.

These simulations are also consistent with the *rotation-dependent heat capacity* effect [1]. Since neither temperature nor angular velocity are constant under compression, the spinning parameter $\varphi = m\omega^2 r_0^2/2T$ varies in time. Hence, in transiting from one equilibrium to another, an average heat capacity can be estimated. Here, the initial equilibrium has $\varphi_0 = 2.740$ at initial temperature $T_0 = 0.501$, while the final equilibrium (after compression) has $\varphi_f = 1.470$ at temperature $T_f = 1.233$. The energy per particle in bringing the system from the initial state to the final state was $\Delta E = 1.232$ (tem-

peratures and energy here are dimensionless). The additional heat-capacity term, $B(\varphi_f)$, depends on the spinning parameter. It represents the energy in the spinning under compression [1] and can be estimated using $(c_v + B)(T_f - T_0) = \Delta E$. For monotomic ideal gas with $c_v = 1.5$, we find $B = 0.168$, intermediate between the equilibrium values at the initial state, $B(\varphi_0) = 0.305$, and at the final state, $B(\varphi_f) = 0.119$ [1], as expected since the spinning parameter changes under compression.

V. DISCUSSION

To summarize, a piezothermal effect was identified. The fundamental associated dimensionless coefficient, the temperature differential over the temperature increase, was calculated in various limits. The temperature gradient produced here is remarkably opposite from that found in vortex tubes, which have the coldest flow on axis. Although vortex tubes also exploit rotating gas effects, the temperature differentials occur through different mechanisms, such as by gas leaving the device through counterpropagating flows in the axial direction, by turbulence, or by frictional forces.

As a matter of fact, the piezothermal effect identified here can also produce cold flow on axis, since the effect changes sign with expansion rather than compression. Thus, axial expansion of spinning gas produces the coldest point on axis. Similarly, lateral expansion of the gas in a gravitational field produces a temperature differential with the bottom hottest.

The piezothermal effect might also be run in reverse; a temperature gradient can produce contraction. Thus, imagine, as in Fig. 1, that the upper chamber is heated in less than a sound time, but an equal amount of heat is taken from the bottom chamber. Then, initially, because the force is proportional to the total contained energy, there is no change in the force on the horizontal walls. However, to restore pressure balance, the gas on bottom is compressed, so the partition is lowered, thereby releasing gravitational potential energy, and thus creating more net pressure on the horizontal walls. The reverse effect, producing horizontal constriction, would occur by imposing the opposite temperature differential.

It can now be appreciated how deep is the analogy to the piezoelectric effect in the limit of compression slow compared to the sound time. In this limit, a temperature differential develops much as a voltage differential develops in the case of the piezoelectric effect. Moreover, absent dissipation, in both cases the effect is reversible: For the piezothermal effect, it is the flow of heat that leads to dissipation; for the piezoelectric effect, it would be the flow of charge. Finally, in both cases, the effect can also be run in reverse. The analogy is not quite as complete in the limit of fast compression, where the temperature is sensitive to the precise time history; however, it might also be surmised that a counterpart to this inertial effect might be found within the piezoelectric effect.

What is particularly fascinating about this piezothermal effect is that it is generalizable to compression under any potential and to multiple gas constituents; we considered here both gravitational and centrifugal potential, but for a single gas constituent. To see the possibilities in more general cases, consider, for example, that, under an electric potential, oppositely charged molecules experience opposite forces. If the temperature equilibration between the species takes longer than the sound time, then this can lead to interesting effects. Consider then a column of plasma, in a vertical potential, such as would occur in the region of a plasma sheath. Upon lateral compression, a vertical temperature differential will develop, but, interestingly, this differential might be opposite for electrons and ions. More generally yet, it is hoped that the identification and elucidation here in special cases in a variety of limits of the piezothermal effect will lead to variations and elaborations on this effect in a variety of physical contexts.

ACKNOWLEDGMENTS

[1] V. I. Geyko and N. J. Fisch, Phys. Rev. Lett. **110**, 150604 (2013).

[2] A. A. Vives, *Piezoelectric Transducers and Applications* (Springer, New York, 2004), Chap. 1.

[3] V. I. Geyko and N. J. Fisch, Phys. Rev. E **90**, 022139 (2014).

[4] C. M. Gao, K. J. Bosschaart, J. C. H. Zeegers, and A. T. A. M. de Waele, Cryogenics **45**, 173 (2005).

[5] R. Liew, J. C. H. Zeegers, J. G. M. Kuerten, and W. R. Michalek, Phys. Rev. Lett. **109**, 054503 (2012).

[6] B. K. Ahlborn and J. M. Gordon, J. Appl. Phys. **88**, 3645 (2000).

[7] J. Bore, S. Maurel, and R. Bazile, Phys. Fluids **14**, 2543 (2002).

[8] J. F. Griffiths, Q. Jiao, M. Schreiber, J. Meyer, and K. F. Knoche, *Proceedings of the Twenty-Fourth Symposium (International) on Combustion* (Combustion Institute, Pittsburgh, PA, 1992), p. 1809.

[9] J. S. Marshall and S. Krishnamoorthy, J. Fluid Mech. **351**, 41 (1997).

[10] J.-P. Racz and J. F. Scott, J. Fluid Mech. **595**, 265 (2008).

[11] L. C. Fai and G. M. Wysin, *Statistical Thermodynamics: Understanding the Properties of Macroscopic Systems* (CRC Press, Boca Raton, FL, 2012), Chap. 9.

[12] G. A. Bird, *Molecular Gas Dynamics and the Direct Simulation of Gas Flows* (Clarendon Press, Oxford, 1994), Chap. 11.

[13] J. E. Dec, Proc. Combust. Instit. **32**, 2727 (2009).

[14] A. E. Hershey and R. F. Paton, Univ. Illinois Bull. **31**, 262 (1933), https://www.ideals.illinois.edu/bitstream/handle/2142/4561/engineeringexperv00000i00262_tei.xml?sequence=3.